CHEMISTRY OF MATERIALS

Communication

pubs.acs.org/cm

New Porous Crystals of Extended Metal-Catecholates

Mohamad Hmadeh,[†,‡] Zheng Lu,[†,‡] Zheng Liu,[§] Felipe Gándara,[†,‡] Hiroyasu Furukawa,[†,‡] Shun Wan,[†,‡] Veronica Augustyn,[⊥] Rui Chang,[⊥] Lei Liao,[‡] Fei Zhou,[⊥] Emilie Perre,[⊥] Vidvuds Ozolins,[⊥] Kazu Suenaga,[§] Xiangfeng Duan,[‡] Bruce Dunn,[⊥] Yasuaki Yamamto,[∥] Osamu Terasaki,[#,□] and Omar M. Yaghi*[,†,‡,#,¶]

[†]Center for Reticular Chemistry, Center for Global Mentoring, [‡]Department of Chemistry and Biochemistry, and [⊥]Department of Materials Science and Engineering, University of California, Los Angeles, California 90095, United States

[§]Nanotube Research Center, AIST, Tsukuba 305-8565, Japan

[∥]SMBU, JEOL Ltd., Akishima, Tokyo 196-8558, Japan

[□]Department of Materials and Environmental Chemistry and EXSELENT, Stockholm University, Stockholm, Sweden

[#]Graduate School of EEWS (WCU), Korea

Supporting Information

KEYWORDS: *metal catecholates, high-resolution transmission electron microscopy, charge storage*

To date, the links of robust and highly porous metal organic frameworks (MOFs) have been largely limited to carboxylate,[1] imidazolate,[2] other azolates,[3] or sulfonate.[4] Although catecholate organic units are well-known and are employed heavily for metal chelation in biology,[5] only the simple 1,2,4,5-tetrahydroxybenzene ($H_6C_6O_4$)[6] or 1,4-dihydroxy-benzoquinone and their homologues ($H_2C_6X_2O_4$, e.g., X = Cl, Br, NO_2 and CH_3) have been explored and incorporated into extended frameworks (Scheme S1 in the Supporting Information).[7] Herein, we describe linking the highly conjugated tricatecholate, 2,3,6,7,10,11-hexahydroxytriphenylene ($H_{12}C_{18}O_6$, HHTP), with Co(II) and Ni(II) ions into two-dimensional porous extended frameworks. These new crystalline materials, termed metal-catecholates (M-CATs), were characterized by X-ray diffraction techniques (single crystal for Co-CAT-1, and powder for Ni-CAT-1) and high-resolution transmission electron microscopy (HR-TEM) studies (for Ni-CAT-1). We demonstrate their high chemical stability (in aqueous and non-aqueous media), thermal stability, and porosity. Cu-CAT-1 microcrystalline material showed high electrical conductivity and charge storage capacity.

CATs were prepared by combining 1 equivalent of HHTP with 2 equivalents of the respective metal(II) acetate hydrated in an aqueous solution, and heating at 85 °C for 24 h to give needle-shaped crystals. The original size of these crystals was too small to be measured by single-crystal X-ray diffraction; however, by slightly varying the synthetic conditions of Co-CAT-1 through the addition of 10% of 1-methyl-2-pyrrolidone (NMP), larger crystals suitable for X-ray crystallography were obtained (see the Supporting Information). The single-crystal X-ray diffraction study of the as-synthesized Co-CAT-1 was carried out using synchrotron radiation in the beamline 24-ID-C at NECAT, in the Advanced Photon Source (APS) at Argonne National Laboratory. The crystal structure was solved in the trigonal space group, $P\bar{3}c1$. There are two crystallographically independent metal atoms, each in an octahedral coordination environment. One of these metal atoms is coordinated to two adjacent deprotonated HHTP linkers and two water ligands to complete the octahedral coordination sphere, which results in the formation of an extended 2D framework. Conversely, the second metal atom is coordinated to only one HHTP linker and to four water ligands giving rise to discrete complexes composed of $Co_3(HHTP)(H_2O)_{12}$. As a result, the structure of Co-CAT-1 comprises two distinct types of alternatively stacked layers (Figure 1A). The first layer is an extended honeycomb structure with hexagonal pores (Figure 1B), and the second layer is formed by the discrete units (Figure 1C) described above. The two axial water ligands participating in the formation of these discrete complexes are hydrogen bonded to oxygen atoms of the HHTP in the adjacent layers. These hydrogen bonds, accompanied by $\pi-\pi$ interactions, create a distortion of the overall structure, leading to corrugated hexagonal layers (Figure 1D). The layers stack in an eclipsed fashion with the HHTP molecules in each layer rotated 60° with respect to each other. A hexagonal array of 1D pore with a 12 Å diameter is thus formed.

HHTP is a redox-active linker that can undergo reversible interconversions between catecholate, semiquinonate and quinone forms.[8] On the basis of the charge balance, the oxidation state of the deprotonated HHTP in the covalently extended first type of layers ($Co_3(HHTP)_2(H_2O)_6$) is −3, which suggests that each of the three dioxolene fragments is in the semiquinone oxidation level. In order to confirm the existence of these monoanionic semiquinonate units within the structure of Co-CAT-1, an electron paramagnetic resonance (EPR) study was performed on the Co-CAT-1 crystals at room temperature. The resulting spectrum displays a near-symmetric signal at g = 2.105 (see Figure S1 in the Supporting Information) which is a characteristic feature of a ligand-centered monoradical. This value is in perfect agreement with

Received: April 19, 2012
Revised: August 22, 2012
Published: August 28, 2012

dx.doi.org/10.1021/cm301194a | *Chem. Mater.* 2012, 24, 3511−3513

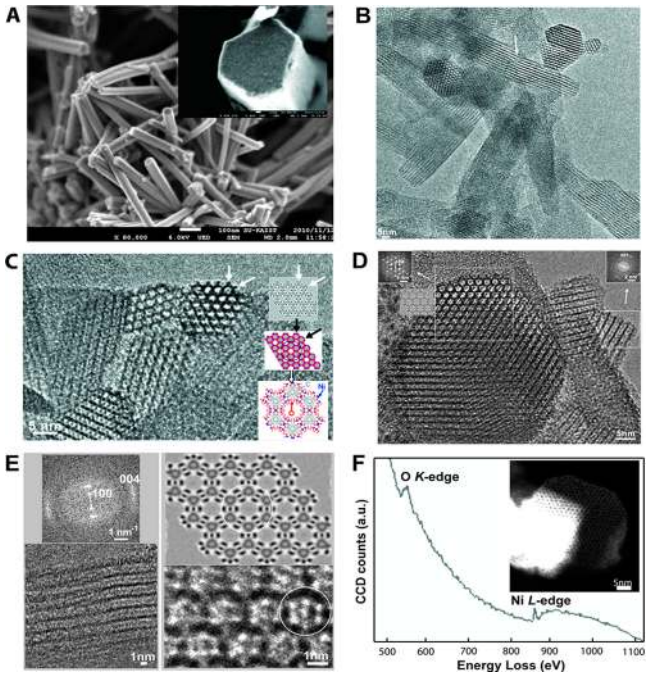

Figure 1. (A) FE-SEM image of Ni-CAT-1 showing uniform rods; inset: zoom in showing the hexagonal shaped surface. (B) Low-magnification HRTEM image of the activated Ni-CAT-1 taken at 120 kV. (C) High-magnification HRTEM image showing the terminal structure of activated Ni-CAT-1 as indicated by arrows. (D) High-magnification HR-TEM image of Ni-CAT-1 taken at 120 kV, the inset images are the fast Fourier transform (FFT) analysis of the corresponding areas indicated by arrows. (E) FFT image demonstrating the wavy characterization of the edges perpendicular to the pore walls and the comparison between the HRTEM and simulated images looking through the [001] direction is shown on the right. (F) Electron energy loss spectroscopy (EELS) spectrum with the annular dark-field scanning transmission electron microscopy (ADF-STEM) image taken under 60 kV shown in the inset.

those obtained for related semiquinonate based complexes.[7,9] For the discrete complexes, $Co_3(HHTP)(H_2O)_{12}$, a −6 oxidation state is required for HHTP in order to compensate the respective charges, suggesting that the metal cations (Co(II)) are coordinated to dianionic catecholate units of the HHTP linker.

As-synthesized crystals of Ni-CAT-1 were not of suitable size for single crystal X-ray analysis. Nevertheless, a Rietveld refinement of Ni-CAT-1 was performed using its powder diffraction pattern data collected with synchrotron radiation, employing the atomic coordinates obtained from the single crystal data of Co-CAT-1. The refinement converged with excellent residual values (R_{wp} = 8.54%, R_p = 6.33), demonstrating that Co and Ni-CAT-1 have the same structure (see Figures S2 and S3 in the Supporting Information).

The crystal structure of Ni-CAT-1 was examined by high-resolution transmission electron microscopy (HRTEM). Initially, low voltage high-resolution scanning electron microscope images of an activated Ni-CAT-1 sample were taken at low landing energy of electrons (1 keV and 400 eV for low magnification and high magnification images, respectively). The images showed uniform morphology with hexagonal rods whose lengths are less than 10 μm and widths are only around 100 nm (Figure 2A). The low magnification HRTEM image of the activated Ni-CAT-1 was taken at 120 kV (Figure 2B). In

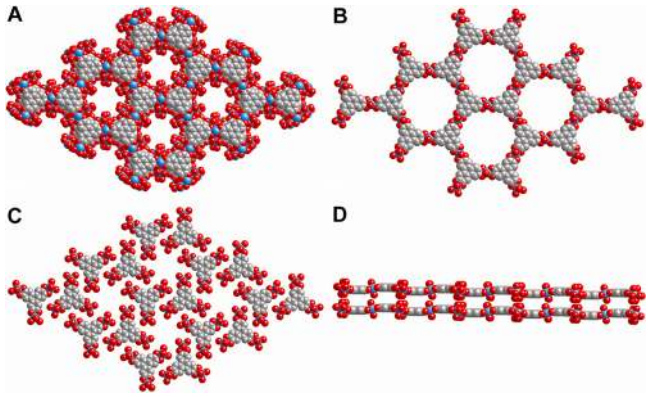

Figure 2. Space filling drawings of the single-crystal structure of Co-CAT-1. (A) View of the Co-CAT-1 structure along the *c* axis. (B) Extended layer of Co-CAT-1. (C) Layer formed by the trinuclear complexes $Co_3(HTTP)(H_2O)_{12}$ (D) View of the two extended corrugated layers along the [110] direction. Color code: Co, blue; C, gray; O, red. Hydrogen atoms are omitted for clarity.

this image, both the channel direction (incident electron beam perpendicular to the channels) and the channel arrangement of a uniform honeycomb structure (incident electron beam parallel to the channels) were observed with some defects identified as indicated by the arrow.

Although HRTEM is a powerful method for the determination of surface structures in inorganic porous materials,[10] this is the first example where HRTEM images provide basic structural information and furthermore the terminal structure of a crystalline MOF is observed. In this exceptional case, the terminal structure of activated Ni-CAT-1 can be clearly observed (Figure 2C). The simulated image of Ni-CAT-1 (Figure 2C, E) show some differences when compared to the real images. Differences in contrast are observed in the area assigned to the position of the metal atoms of the interlayer complexes. This fact suggests small changes probably in the orientation of the complexes after the activation process and under the acquisition conditions (high vacuum) for the HRTEM image. The HRTEM images were accompanied by a fast Fourier transform (FFT) analysis, which allowed the determination of the unit cell lattice parameter of a = 2.02 nm (Figure 2D). This finding is in agreement with the value obtained from the single crystal data analysis of Co-CAT-1 (a = 2.21 nm) and the one obtained from the X-ray powder diffraction study of Ni-CAT-1 (a = 2.19 nm). The arc line reflection shown in the FFT image in the inset of Figure 2E demonstrates the wavy characterization of the fringes perpendicular to the pore walls, indicating the fluctuation of the Ni atoms. The spacing between these wavy fringes, calculated from the FFT images, is about 0.32 nm, which corresponds to the interlayer distance (0.33 nm obtained from the X-ray data).

It is a challenge to observe MOFs by using scanning transmission electron microscopy (STEM) due to a focused beam that has a higher beam density than in transmission electron microscopy (TEM) mode. Typically, zeolites and mesoporous silicas are damaged much faster in STEM mode than in conventional TEM mode. Remarkably, for the first time we were able to overcome this challenge and observe a crystalline MOF material by using STEM. In this study a JEOL 2100F with a cold field-emission gun equipped with a newly designed aberration corrector (the DELTA-corrector) was

dx.doi.org/10.1021/cm301194a | *Chem. Mater.* 2012, 24, 3511−3513

operated at 60 kV. A Gatan GIF Quantum was used for the electron energy loss spectroscopy (EELS) chemical analyses. The inner and outer collection angles for the annular dark-field (ADF) image were 58 and 130 mrad, respectively. The beam current was 10 pA for the ADF imaging and the EELS chemical analysis. The honeycomb structure of Ni-CAT-1 is clearly observed in the STEM image, albeit at the expense of structural electron beam stability, which collapsed after the whole scan was complete. EELS profile showed Ni (*L*-edge) and O (*K*-edge) (Figure 2F).

To assess the porosity and the architectural stability of the M-CATs, Ar gas adsorption measurements at 87 K were performed (see the Supporting Information). The Brunauer–Emmett–Teller (BET) surface areas for Co and Ni-CAT-1 were calculated to be 490 and 425 $m^2\ g^{-1}$, respectively.

The electrical conductivity of CATs was measured at room temperature on single crystals of Cu-CAT-1 using a four-point probe method with Au electrodes as contact material (see the Supporting Information). The conductance of two different crystals of Cu-CAT-1 was calculated to be 1.8×10^{-1} and 2.1×10^{-1} S cm^{-1}, respectively, which is more than 1 order of magnitude higher than a previously reported value for an iodine-loaded MOF.[11] Other reports on the electrical conductivity measurements of MOFs showed much lower conductivity values, because these measurements were performed using compressed pellets.[12] Indeed, the electrical conductivity of single crystal is always higher than the polycrystal conductivity of the same material. Therefore, it is not appropriate to compare these values to that of Cu-CAT-1.[13] Preliminary electrochemical measurements of Cu-CAT-1 were also performed using different nonaqueous electrolytes. Cyclic voltammetry measurements reveal that there are several reversible redox peaks, indicating that Cu-CAT-1 can be utilized as an electrochemical energy storage material. Indeed, after 50 charge–discharge cycles, Cu-CAT-1 exhibits a lithium-ion capacity of 284 C g^{-1} (80 mA h g^{-1}). This capacity value is greater than the previously reported one for another MOF (MIL-53) at similar time scales.[14] We believe that our initial findings with CATs pave the way for the design of new energy storage materials.

■ ASSOCIATED CONTENT

Supporting Information

Full synthetic and analytic details, including crystallographic information files (CIFs). This material is available free of charge via the Internet at http://pubs.acs.org.

■ AUTHOR INFORMATION

Corresponding Author

*E-mail: yaghi@berkeley.edu.

Present Address

[¶]Department of Chemistry, University of California, and The Molecular Foundry, Division of Materials Sciences, Lawrence Berkeley National Laboratory, Berkeley, California 94720, United States

Notes

The authors declare no competing financial interest.

■ ACKNOWLEDGMENTS

This material is based on work supported as part of the Molecularly Engineered Energy Materials, an Energy Frontier Research Center funded by the U.S. Department of Energy (DOE), Office of Science, Office of Basic Energy Sciences, under Award DE–SC0001342. This research used resources of the National Energy Research Scientific Computing Center (NERSC). We gratefully acknowledge Dr. Duilio Cascio (UCLA–DOE Institute of Genomics and Proteomics) for experimental assistance. We thank M. Capel, K. Rajashankar, F. Murphy, J. Schuermann, and I. Kourinov at NE–CAT beamline 24–ID–C at APS, which is supported by National Institutes of Health Grant RR–15301. F.G. acknowledges funding by the Spanish Ministry of Education through the "Programa de Movilidad de Recursos Humanos del Plan Nacional de I–D+i 2008–2011." WCU (R–31–2008–000–10055–0) for OT and OM and EXSELENT, Stockholm University for OT are acknowledged for funding.

■ REFERENCES

(1) Furukawa, H.; Ko, N.; Go, Y. B.; Aratani, N.; Choi, S. B.; Choi, E.; Yazaydin, A. O.; Snurr, R. Q.; O'Keeffe, M.; Kim, J.; Yaghi, O. M. *Science* **2010**, *329*, 424.

(2) Banerjee, R.; Phan, A.; Wang, B.; Knobler, C.; Furukawa, H.; O'Keeffe, M.; Yaghi, O. M. *Science* **2008**, *319*, 939.

(3) Zhang, J. P.; Zhang, Y. B.; Lin, J. B.; Chen, X. M. *Chem. Rev.* **2012**, *112*, 1001.

(4) Côté, A. P.; Shimizu, G. K.H. *Coord. Chem. Rev.* **2003**, *245*, 49.

(5) (a) Sandy, M.; Butler, A. *Chem. Rev.* **2009**, *109*, 4580. (b) Zanello, P.; Corsini, M. *Coord. Chem. Rev.* **2006**, *250*, 2000.

(6) Nakabayashi, K.; Ohkoshi, S. *Inorg. Chem.* **2009**, *48*, 8647.

(7) (a) Kitagawa, S.; Kawata, S. *Coord. Chem. Rev.* **2002**, *224*, 11. (b) Abrahams, B. F.; Hudson, T. A.; McCormick, L. J.; Robson, R. *Cryst. Growth. Des.* **2011**, *11*, 2717.

(8) Barthram, A. M.; Cleary, R. L.; Kowallick, R.; Ward, M. D. *Chem Commun* **1998**, 2695.

(9) Grange, C. S.; Meijer, A. J. H. M.; Ward, M. D. *Dalton Trans.* **2010**, *39*, 200.

(10) (a) Ohsuna, T.; Horikawa, Y.; Hiraga, K.; Terasaki, O. *Chem. Mater.* **1998**, *10*, 688. (b) Liu, Z.; Ohsuna, T.; Terasaki, O.; Camblor, M. A.; Diaz–Cabanas, M. J.; Hiraga, K. *J. Am. Chem. Soc.* **2001**, *123*, 5370.

(11) Zeng, M. H.; Wang, Q. X.; Tan, Y. X.; Hu, S.; Zhao, H. X.; Long, L. S.; Kurmoo, M. *J. Am. Chem. Soc.* **2010**, *132*, 2561.

(12) (a) Takaishi, S.; Hosoda, M.; Kajiwara, T.; Miyasaka, H.; Yamashita, M.; Nakanishi, Y.; Kitagawa, Y.; Yamaguchi, K.; Kobayashi, A.; Kitagwa, H. *Inorg. Chem.* **2008**, *48*, 9048. (b) Kobayashi, Y.; Jacobs, B.; Allendorf, M. D.; Long, J. R. *Chem. Mater.* **2010**, *22*, 4120. (c) Avendano, C.; Zhang, Z.; Ota, A.; Zhao, H.; Dunbar, K. R. *Angew. Chem., Int. Ed.* **2011**, *50*, 6543. (d) Gándara, F.; Uribe-Romo, F. J.; Britt, D. K.; Furukawa, H.; Lei, L.; Cheng, R.; Duan, X.; O'Keeffe, M.; Yaghi, O. M. *Chem.—Eur. J.* **2012**, *18*, 10595.

(13) Schulgasser, K. *J. Appl. Phys.* **1975**, *47*, 1880.

(14) Férey, G.; Millange, F.; Morcrette, M.; Serre, C.; Doublet, M. L.; Grenèche, J. M.; Tarascon, J. M. *Angew. Chem., Int. Ed.* **2007**, *46*, 325.

■ NOTE ADDED AFTER ASAP PUBLICATION

This paper was published ASAP on August 31, 2012, with a spelling error in an author's name and an incorrect version of the Supporting Information. These items were corrected in the version published ASAP on September 5, 2012. An additional author was added to the version published ASAP September 10, 2012.